Environment International 204 (2025) 109823

Contents lists available at ScienceDirect

Environment International

journal homepage: www.elsevier.com/locate/envint

Full length article

Short-term effects of ultrafine particles on stroke events: an assessment using four different exposure metrics

Minqi Liao [a,b,c,*], Siqi Zhang [a,d], Maximilian Schwarz [a], Cheng He [a], Susanne Breitner-Busch [a,b], Josef Cyrys [a], Markus Naumann [e], Lino Braadt [e], Claudia Traidl-Hoffmann [f,g,h], Gertrud Hammel [i], Annette Peters [a,b,j], Michael Ertl [e,k,1], Alexandra Schneider [a,1]

[a] Institute of Epidemiology, Helmholtz Zentrum München - German Research Center for Environmental Health (GmbH), Neuherberg, Germany
[b] Institute for Medical Information Processing, Biometry, and Epidemiology, IBE, Medical Faculty, Ludwig-Maximilians-Universität München, Munich, Germany
[c] Pettenkofer School of Public Health, Munich, Germany
[d] Department of Environmental Health Sciences, Yale School of Public Health, New Haven, CT, USA
[e] Neurology and Clinical Neurophysiology, University Hospital Augsburg, Augsburg, Germany
[f] Institute of Environmental Medicine and Integrative Health, Medical Faculty, University of Augsburg, Augsburg, Germany
[g] CK-CARE, Christine Kühne, Center for Allergy and Research and Education, Davos, Switzerland
[h] Institute of Environmental Medicine, Helmholtz Zentrum München - German Research Center for Environmental Health, Neuherberg, Germany
[i] Institute for Social Sciences, Sociology and Health Research, University of Augsburg, Augsburg, Germany
[j] Munich Heart Alliance, German Center for Cardiovascular Health (DZHK e.V., partner-site Munich), Munich, Germany
[k] Clinic for Neurology and Neurological Rehabilitation, District Hospital Günzburg, Günzburg, Germany

ARTICLE INFO

Handling Editor: Hanna Boogaard

ABSTRACT

Background: The effects of different ultrafine particle (UFP) metrics on strokes are unclear. This case-crossover study investigated the association between short-term exposure to four size-segregated UFP metrics and stroke occurrence.

Methods: From 2006 to 2020, we included 19,518 stroke cases from the University Hospital Augsburg, Germany, a less polluted area. Meanwhile, daily averages of four UFP metrics, including particle number (PNC), mass (PMC), length (PLC), and surface area (PSC) concentrations, were collected from fixed monitoring sites in Augsburg. Conditional logistic regression was employed to assess the association between UFP metrics and stroke risk. Potential individual vulnerability and effect modification were examined using the stratified and interaction analyses.

Results: Elevated risk of stroke events was largely similar across all four UFP metrics. The odds ratios (95 % confidence intervals) of strokes for each interquartile range increase in lag 0–6 days of UFPs were 4.76 % (1.06; 8.60) for PNC, 3.99 % (0.93; 7.13) for PMC, 4.52 % (1.11; 8.05) for PLC, and 4.14 % (1.00; 7.38) for PSC. Stable associations with strokes were mainly found for the size fractions of 10–100 nm and 30–100 nm. The cumulative effects of UFP were more pronounced for ischemic strokes and minor strokes with a lower severity. Cold spells might exaggerate the effects of UFPs.

Conclusion: UFP metrics like particle length and surface area concentration, aside from particle number, may provide valuable insights into particle properties relevant to stroke risk. Expanding real-time, size-segregated monitoring of UFPs represents an effective strategy to mitigate the health impacts of traffic-related air pollution.

* Corresponding author at: Institute of Epidemiology, Helmholtz Zentrum München-Deutsches Forschungszentrum für Gesundheit und Umwelt (GmbH), Ingolstädter Landstraße 1, D-85764 Neuherberg, Germany.
E-mail address: minqi.liao@campus.lmu.de (M. Liao).
[1] These authors contributed equally to this work.

https://doi.org/10.1016/j.envint.2025.109823
Received 17 June 2025; Received in revised form 10 September 2025; Accepted 26 September 2025
Available online 28 September 2025

1. Introduction

According to the Health Effects Institute, air pollution accounted for 8.1 million deaths in 2021, making it the second-largest risk factor of death worldwide (Health Effects Institute, 2024). Increasing epidemiological evidence has indicated the short-term adverse health impacts of ambient particulate matter (PM) exposure, such as increased hospital admissions (Kim et al., 2015) and mortality (Yu et al., 2024), particularly for cardiovascular and respiratory diseases (Sun et al., 2024; Ban et al., 2024; Gouveia et al., 2024). Ultrafine particles (UFPs), which have a diameter of 0.1 μm or less (≤ 100 nm), are typically generated as by-products of fossil fuel combustion and emissions from motor vehicles (HEI Review Panel on Ultrafine Particles, 2013). UFPs have emerged as one of the greatest concerns for human health due to their unique properties, characterized by their low mass but high number and surface area concentration (HEI Review Panel on Ultrafine Particles, 2013; Oberdörster et al., 2005; Peters et al., 2011). Their motion is mainly defined by diffusion, allowing UFPs to effectively deposit in the alveolar regions of the lungs, while they are less likely to deposit in the larger airways (Peters et al., 2011). This capability enables UFPs to translocate into cells and reach other organs in the body (HEI Review Panel on Ultrafine Particles, 2013; Peters et al., 2011). Furthermore, their large active surface makes them more threatening by absorbing greater quantities of hazardous metals and organic compounds (Oberdörster et al., 2005). These distinct UFP properties make it possible to determine toxicity more accurately and offer practical alternative ways to regulate and monitor reflectors by considering different UFP metrics. Specifically, UFPs are mainly measured as particle number concentration (PNC, number of particles/cm^3), as they constitute 85 % or more of the total number of fine particulate matter (e.g., with a diameter of ≤2.5 μm; $PM_{2.5}$) (Hinds, 1982), but contribute little to the particle mass concentrations (PMC, μg/m^3) in ambient air (HEI Review Panel on Ultrafine Particles, 2013). Besides, particle surface area concentration (PSC, $\mu m^2/cm^3$) considers the absorption and retention of toxic substances and plays an important role in determining the biological activity of nanoparticles (Sager and Castranova, 2009).

Studies have shown an association between short-term exposure to UFPs and adverse health effects, such as myocardial infarction (MI) risk (Chen et al., 2020; Jiang et al., 2023; Wolf et al., 2015; Hu et al., 2020), cardiovascular hospitalizations (Lin et al., 2022), and even mortality (Lin et al., 2022; Lanzinger et al., 2016; Wichmann et al., 2000; Bergmann et al., 2023; Schwarz et al., 2023). The difference in physical properties of various UFP-related metrics may influence their health effects; however, evidence on the impact of different UFP metrics on well-being has remained insufficient. A case-crossover study reported that daily UFP exposure, measured using PNC, over the previous four days (0–4) was associated with increased hospital admissions for ischemic stroke in Copenhagen, Denmark (Andersen et al., 2010). Another case-crossover study in New York State, U.S., also noticed an association between UFP exposure, measured using PSC, and elevated stroke risk, with PSC showing to be a more sensitive indicator than PNC (Lin et al., 2022). Furthermore, compared to PNC, the particle length concentration (PLC, mm/cm^3) was found to be a UFP metric being more closely associated with blood inflammatory biomarkers in blood (Rückerl et al., 2016) and the risk of MI in Augsburg, Germany (Chen et al., 2020).

Within the conventional size range of ≤100 nm, the size fractions of UFPs in urban environments can be related to the nature of the fuel and the processes by which they are typically formed, specifically, the primary particles emitted directly from the engine (>30 nm). In particular, the secondary particles (newly formed nucleation mode, <30 nm) are a considerable number of very small particles formed after cooling and condensation of exhaust gases (Morawska et al., 2008), and the Aitken mode (30–100 nm) is typically associated with combustion sources (Lin et al., 2025). Both modes contribute to the concentration of traffic-related peaks during rush hour (Lin et al., 2025). The accumulation mode (100–1000 nm) commonly results from the emissions of fine particles and dynamic events, including condensation and coagulation (Kwon et al., 2020). Epidemiological evidence, however, focusing on the effects of size-segregated UFP metrics is limited. Additionally, outdoor air temperature was found to be associated with adverse cardiovascular outcomes, such as increased blood pressure (Chen et al., 2015). Similarly, our previous research has revealed that nocturnal heat exposure is related to elevated stroke risk (He et al., 2024). Cold spells were associated with an increased risk of hospitalization for MI (Ni et al., 2024). Furthermore, studies unveiled that heat waves interact synergistically with $PM_{2.5}$, increasing the mortalities of MI (Xu et al., 2023) and strokes (Deng et al., 2024). No evidence exists for the potential influence of extreme temperature events (ETEs), including heat waves and cold spells, on the association between UFPs and strokes.

Using four UFP metrics of different size fractions, this study aims to distinguish the association between various UFPs and stroke events using daily hospitalization data collected over a study period of 15 years in Augsburg, Germany, in which monitoring stations were designed for the collection of several physical and chemical particulate characteristics (Rückerl et al., 2016). Additionally, we estimated the effects across stroke subtypes, disabilities, and severities and explored the potential modification effect by time-invariant factors (sex assigned at birth, age), seasons, time trends, and ETEs.

2. Materials and methods

2.1. Study population

We used the first stroke events that occurred during the study period (between January 1st, 2006, and August 31st, 2020) at the University Hospital Augsburg. This is one of the biggest stroke centers in Germany and is responsible for more than 750,000 inhabitants in the region (He et al., 2024). This study was performed following the Declaration of Helsinki. Ethical approval was waived in the present study according to the Bavarian Hospital Act.

2.2. Outcome and covariates

Based on the records from this comprehensive stroke care facility, we collected demographic characteristics (sex and age) and basic clinical data of patients (subtypes of strokes, disability, and severity) at admission. The following three main subtypes of strokes were defined according to the International Statistical Classification of Diseases and Related Health Problems, 10th version (ICD-10 codes): transient ischemic attacks (TIAs) (G45), hemorrhagic strokes (I60, I61, I62), and ischemic strokes (I63). Following the occurrence of a stroke, we measured functional independence using the Modified Rankin Scale (mRS), a 7-level scale ranging from 0 (no symptoms) to 6 (death) (Rankin, 1957; Kasner, 2006). Besides, a severe stroke was represented by a higher score on the National Institutes of Health Stroke Scale (NIHSS), a scale of 0 to 42 that assessed the stroke severity (Kasner, 2006). To simplify the analysis, we defined "Disability due to strokes" by combining an mRS score of 0–2 as "No symptoms to slight disability" with an mRS score of 3–6 as "Moderate disability to death". Furthermore, we calculated the "Stroke severity" by combining the NIHSS scores of 0–3 and 4–42 as "No symptoms to minor stroke" and "Moderate to severe stroke", respectively.

2.3. Exposures

2.3.1. Air pollution and meteorological data

The UFP measurements have been conducted since 2004 at a fixed urban background site on the premises of the Fachhochschule Augsburg (FH, University of Applied Sciences Augsburg) in Augsburg, Germany, and were available for the whole study period. The daily average concentrations of the four metrics of UFPs, including particle number

(PNC), mass (PMC), length (PLC), and surface area (PSC) concentrations, were obtained from this aerosol monitoring station located 1 km southeast of the city center, with the nearest major road in the northeast at a distance of 100 m (Cyrys et al., 2008). The supplemental materials section I explains details regarding the devices for collecting and the calculation methods for the four different UFP metrics.

Based on the particle behavior, origin, and deposition in the respiratory tract (Wichmann et al., 2000), we mainly focused on four metrics within the size of ≤100 nm, the typical range of UFPs by convention (Wichmann et al., 2000). We excluded the ultra-small UFPs of 3–10 nm from our analysis and primarily examined the 10–100 nm range to avoid the influence of the substantially increased probability of measurement uncertainty for particles below 10 nm in size (Zhang and Flagan, 1996) and to keep our findings comparable with others. In addition, we further subdivided the particle size distribution into the following ranges: 10–30 nm (nucleation mode) and 30–100 nm (Aitken mode) due to their likely deposition in the lung (Chen et al., 2020). Particles of 100–500 nm are more likely to deposit in the lung than those of >500 nm, which tend to deposit more in the upper respiratory tract (Gu et al., 2012). Particles of 100–500 nm (accumulation mode) and 10–500 nm (total measured particle range) were therefore included in the analysis to further capture the influence of UFPs in a larger size range and to explore the combined exposure to all measured particles.

Classic air pollutants were routinely measured at different monitoring sites for specific study periods (Yao et al., 2023), owing to different operating periods across monitoring sites. In detail, the continuous levels of PM with an aerodynamic diameter of ≤ 10 μm (PM_{10}) and $PM_{2.5}$ and meteorological parameters (ambient air temperature and relative humidity) were obtained from the FH measuring site throughout the whole study period (2006–2020). The 24-hour average nitrogen oxides (NO_2, NO) were obtained from an urban background monitoring site at Bourgesplatz (BP), located approximately 1.5 km north of the city center of Augsburg (Yao et al., 2023). The daily average ozone (O_3) level was measured at the monitoring site operated by the Bavarian Environment Agency (LfU), which is located 4 km south of the city center (Yao et al., 2023). Specifically, missing PM_{10} and $PM_{2.5}$ values were imputed from existing LfU or BP data, while missing NO and NO_2 values were imputed from measurements at the LfU.

2.3.2. ETE definitions

Considering that ambient air temperature plays a role in concentrations of UFP, from the perspective of PNC (Morawska et al., 2008), we defined the ETEs (heat waves or cold spells) with a combination of intensity and duration of extreme air temperatures according to the relative threshold approach (Xu et al., 2023; Deng et al., 2024). We then calculated the specific cutoffs of air temperature for heat waves (95.0th and 97.5th percentiles) and cold spells (2.5th and 5.0th percentiles). Days with air temperature equaling or exceeding any of the heat wave cutoffs were considered heat waves, whereas days with air temperature equaling or below any of the cold spell cutoffs were considered cold spells. In each definition of ETEs, the heat waves and the cold spells were coded as "1″ and "2", respectively, while the remaining non-ETE days with normal air temperature were coded as "0" (Xu et al., 2023; Deng et al., 2024). The details of air temperature thresholds and the number of ETE days in different ETE definitions are provided in sTable 1 in the supplementary materials-section II.

2.4. Statistical analysis

A time-stratified case-crossover design was applied to explore the association between four UFP concentration metrics and stroke events. The case day referred to the date of hospital admission owing to stroke events, and the corresponding control days were defined as dates on the identical day of the week and in the same calendar month as the case day, with each patient serving as his or her own control (Janes et al., 2005). The case-crossover study design controls for time-invariant confounding (e.g., sex, age, family history, and genetic variations) by making within-subject comparisons within reference windows (Janes et al., 2005). In addition, choosing the control days close to the case days enabled us to control for various time-varying variables, such as seasonality and long-term trends in air pollution and stroke events (Janes et al., 2005).

Conditional logistic regression models were implemented by applying a linear term for the four size-segregated UFP metrics during different lag periods in separate models. Effect estimates were reported as the percent changes (PCs) in the odds ratios (ORs) and their corresponding 95 % confidence intervals (CIs) associated with per interquartile range (IQR) increases in UFPs. After excluding the days with missing values of UFP metrics, we explored UFP effects across different exposure windows: i) the single-day lags: current day (lag 0) and up to six days before the events (lag 1-lag 6); ii) the moving average lags: multi-days preceding the events representing immediate (lag 0–1) and delayed (lag 2–4, 5–6); and iii) the cumulative effects (lag 0–6). Using a natural cubic spline with three degrees of freedom (df), our main model further adjusted for the same lag day of ambient air temperature and relative humidity to control for potentially remaining confounding factors.

To identify whether specific subgroups exhibit differential susceptibility, stratified analyses were conducted by fitting separate models by subtypes of strokes (TIAs, hemorrhagic, and ischemic strokes), stroke-induced disability (No symptoms to slight disability [mRS 0–2] *vs.* Moderate disability to death [mRS 3–6]), and severity of stroke (No symptoms to minor stroke [NIHSS 0–3] *vs.* Moderate to severe stroke [NIHSS 4–42]). The nonspecific types of strokes were excluded from the stratified analysis.

To explore potential effect modifications on the associations between UFP exposures and stroke risk, we further included interaction terms in the model, including sex (men *vs.* women), age (<65.0 years *vs.* ≥ 65.0 years), seasons (warm seasons [from May to October] *vs.* cold seasons [from November to April]), and five-year periods of admission (2006–2010, 2011–2015, 2016–2020), which were divided due to their similar time durations and comparable total number of cases. To further assess the potential modification effects of two types of ETEs, the interaction models were also built for heat waves during the warm seasons (non-ETE days *vs.* heat waves) and cold spells during the cold seasons (non-ETE days *vs.* cold spells), respectively.

A series of sensitivity analyses were carried out to test the robustness of our results: i) we fitted the two-pollutant models for investigating the potential independence of the UFP effects by additionally controlling for the same lag day of routinely measured air pollutants ($PM_{2.5}$, PM_{10}, NO, and NO_2), which were selected if they had a Spearman correlation coefficient (rs) < 0.70 and a variance inflation factor (VIF) < 5 to avoid collinearity (Kim, 2019); ii) to assess the potential influence of missing values, the main analysis was repeated after missing values were imputed using the average value of the non-missing values for the same weekday in the neighboring 1-week (one week before and after); iii) we excluded patients who admitted to the hospital after the beginning of the COVID-19 pandemic (February 2020) to avoid the potential fluctuation in ambient air pollution concentrations due to the "lock-down" in Germany; v) according to Stafoggia M, *et al.,* (Stafoggia et al., 2013), we separately adjusted for high and low temperatures, which were defined as the average temperature on the current and previous 1 day before the event (lag 0–1) above the median annual temperature and the average temperature on the previous 6 days (lag 1–6) below the median annual temperature, respectively. The optimal degree for natural cubic splines was set at 3 to allow better comparability when entering different temperatures; v) we plotted the exposure–response curve by introducing a restricted cubic spline function (df = 3) for UFPs in the main model to check the linearity of the association between UFP metrics and the odds of stroke events.

All data management and statistical analyses were conducted using R software (Version 4.1.2). Statistical tests were two-sided, with a

significance level (α) set at 0.05 and a marginal significance at 0.10.

3. Results

3.1. Descriptive statistics

The basic characteristics of the study population by subtypes of strokes are shown in Table 1. Over 15 years, 19,518 patients were admitted to the hospital for a stroke, including 5,024 (25.7 %) TIAs, 1,208 (6.2 %) hemorrhagic strokes, and 13,242 (67.8 %) ischemic strokes, with the remaining 44 (0.2 %) events of unknown stroke type. The mean (SD) age of all patients was 70.9 (13.3) years, with 8,585 (44.0 %) being women. A substantial proportion of patients were ≥ 65.0 years of age (14,030; 73.1 %), and the majority were diagnosed with a "Moderate disability to death [mRS 3–6] (31.8 %) or "No symptoms to minor stroke [NIHSS 0–3]" (42.0 %). Stroke events occurred more often during the cold seasons (60.4 %), the period between 2011 and 2015 (35.7 %), than during the other periods of similar length. The distribution of strokes between heat waves (4.7 %) and cold spells (4.9 %) was even.

The daily means of the four UFP metrics in four size fractions throughout the study period are displayed in Table 2. At the size of 10–100 nm, the mean (SD) exposure concentrations were 7,411.5 (4,370.0) particles/cm^3 for PNC, 0.7 (0.5) μg/m^3 for PMC, 283,123.1 (17,5247.6) mm/cm^3 for PLC, and 46.0 (29.8) μm^2/cm^3 for PSC, respectively. Especially, within the ultrafine range (10–100 nm), a larger contribution from the Aitken mode (30–100 nm) than from the nucleation mode (10–30 nm) was observed among the four UFP metrics. The mean concentrations of PMC and PSC in the accumulation mode (100–500 nm) were notably higher than those of other size fractions. As sTable 2 presents, the distribution of UFPs after imputation was quite similar to the original data. sTable 3 provides the mean levels of the current-day UFP metrics by different definitions of ETEs. Notably, the daily averages of four UFP metrics appeared to be higher during cold spells than during heat waves.

The Spearman correlation coefficients between the four UFPs in four size ranges and two meteorological parameters are shown in sTable 4. Overall, daily UFPs within different size fractions displayed positive correlations with each other (Spearman rs = 0.34 to 0.99) but were predominantly inversely related to ambient air temperature and relative humidity. For each specific UFP metric within the size of 10–100 nm, their correlations with four traditionally measured ambient air pollutant parameters ($PM_{2.5}$, PM_{10}, NO, and NO_2) are provided in sTable 5. In general, there were weak positive correlations (Spearman rs = 0.03 to 0.11) between all four UFP metrics and classical air pollutants.

3.2. Association between daily UFPs and overall stroke events

Fig. 1 describes the associations between daily UFPs within the size of 10–100 nm and the occurrence of overall stroke events across different exposure windows, with the single-day model showing the 3-day transient effects and the lagged moving average model indicating the 2–4 days delayed and 0–6 days cumulative adverse health effects of UFPs on strokes. Particles within the size ranges of 30–100 nm, 100–500 nm, and 10–500 nm also showed similar results; however, the effect of the smallest particles (10–30 nm) tended to occur later (sFigs. 1–4).

For the single-day lags, an elevated risk of stroke events was consistently seen for the exposure window of lag 3 days across all four UFP metrics. An IQR increase in four UFP metrics (10–100 nm) at lag 3-day was associated with an increase in the odds of 2.45 % (0.14; 4.81), 2.54 % (0.26; 4.87), 2.57 % (0.27; 4.92), and 2.57 % (0.29; 4.90), respectively. Compared to the smaller particles in the nucleation mode (10–30 nm), the effect estimates from the Aitken mode (30–100 nm) were larger and more consistently observed across four metrics (see sTable 6). For the moving average lags, we noticed a delayed effect (2–4 days) and a cumulative effect (0–6 days) of all four UFP metrics within

Table 1
Description of stroke patients hospitalized in the study areas of Augsburg, Germany, from 2006 to 2020.

Characteristics	Overall strokes	TIAs [a]	Hemorrhagic strokes [a]	Ischemic strokes [a]
N (%)	19,518	5024 (25.7)	1208 (6.2)	13,242 (67.8)
Age (y), continuous	70.9 ± 13.3	69.06 ± 13.20	71.61 ± 13.54	71.53 ± 13.27
Age (y), categorical				
<65.0	5488 (28.1)	1634 (32.5)	314 (26.0)	3532 (26.7)
≥65.0	14,030 (71.9)	3390 (67.5)	894 (74.0)	9710 (73.3)
Sex				
Men	6290 (32.2)	1535 (30.6)	416 (34.4)	4328 (32.7)
Women	8585 (44.0)	2176 (43.3)	537 (44.5)	5859 (44.2)
Missing	4643 (23.8)	1313 (26.1)	255 (21.1)	3055 (23.1)
Disability due to strokes (by mRS score)				
No symptoms to slight disability [b]	5879 (30.1)	2358 (86.2)	146 (22.1)	3374 (38.8)
Moderate disability to death [c]	6214 (31.8)	378 (13.8)	516 (77.9)	5316 (61.2)
Missing	7425 (38.0)	2288 (45.5)	546 (45.2)	4552 (34.4)
Stroke severity (by NIHSS score)				
No symptoms to minor stroke [d]	8189 (42.0)	2837 (93.5)	271 (35.6)	5070 (51.7)
Moderate to severe stroke [e]	5425 (27.8)	196 (6.5)	490 (64.4)	4733 (48.3)
Missing	5904 (30.2)	1991 (39.6)	447 (37.0)	3439 (26.0)
Seasons [f]				
Warm seasons	9667 (50.0)	2558 (50.9)	581 (48.1)	6512 (49.2)
Cold seasons	9851 (50.0)	2466 (49.1)	627 (51.9)	6730 (50.8)
Extreme temperature events (ETE)				
Heat waves [g]	912 (4.7)	255 (5.1)	32 (2.6)	622 (4.7)
Cold spells [h]	953 (4.9)	240 (4.8)	68 (5.6)	641 (4.8)
Non-ETE days	17,653 (90.4)	4529 (90.1)	1108 (91.7)	11,979 (90.5)
5-year periods [i]				
2006–2010	6649 (34.1)	1825 (36.3)	437 (36.2)	4351 (32.9)
2011–2015	6966 (35.7)	1767 (35.2)	434 (35.9)	4757 (35.9)
2016–2020	5903 (30.2)	1432 (28.5)	337 (27.9)	4134 (31.2)

Note: [a] Types of strokes were defined based on the ICD-10 code; [b] the mRS score of 0–2 is "No symptoms to slight disability"; [c] mRS 3–6 is "Moderate disability to death". [d] NIHSS score of 0–3 is "No symptoms to minor stroke"; [e] NIHSS score of 4–42 is "Moderate to severe stroke"; [f] Seasons: determined by the official time of heating time in Germany, warm seasons: May to October; cold season: November to April; [g] Heat waves are defined as the days with air temperature equaling to or exceeding the 95.0th or 97.5th percentiles; [h] Cold spells are defined as the days with air temperature equaling to or lowering than the 2.5th or 5.0th percentiles; [i] 5-year periods: the year of admission. **Abbreviations**: TIA, Transient ischemic attacks; mRS, Modified Rankin scale (a scale ranging from 0 to 6, with higher scores indicating greater disability); NIHSS, National Institutes of Health Stroke Scale (a scale ranging from 0 to 42, with higher scores indicating greater stroke severity).

Table 2
Basic descriptive statistics of daily levels of four ultrafine particle metrics in five size ranges in the study areas of Augsburg, Germany, from 2006 to 2020.

	N	Missing (%)	Mean ± SD	Min	P25	Median	P75	Max	IQR
PNC (particles/cm^3)									
PNC $_{10\text{-}100}$	5025	454 (8.29)	7411.5±4370.0	504.4	4469.6	6416.7	9021.1	48386.9	4551.5
PNC $_{10\text{-}30}$	5025	454 (8.29)	3438.5±2083.6	279.8	2103.7	2968.4	4230.6	42526.3	2126.9
PNC $_{30\text{-}100}$	5025	454 (8.29)	3973.0±2623.1	224.7	2299.3	3373.6	4866.4	26932.0	2567.1
PNC $_{100\text{-}500}$	5016	463 (8.45)	1490.0±990.0	0.0	843.7	1282.7	1851.5	10562.8	1007.8
PNC $_{10\text{-}500}$	5016	463 (8.45)	8908.3±5116.4	735.9	5498.0	7758.5	10841.0	49795.9	5343.0
PMC (μg/m^3)									
PMC $_{10\text{-}100}$	5025	454 (8.29)	0.7±0.5	0.1	0.4	0.6	0.9	5.1	0.5
PMC $_{10\text{-}30}$	5025	454 (8.29)	0.0±0.0	0.0	0.0	0.0	0.0	0.4	0.0
PMC $_{30\text{-}100}$	5025	454 (8.29)	0.7±0.5	0.0	0.4	0.6	0.9	5.0	0.5
PMC $_{100\text{-}500}$	5016	463 (8.45)	10.1±7.9	0.0	5.1	8.3	12.8	98.8	7.7
PMC $_{10\text{-}500}$	5016	463 (8.45)	10.8±8.2	0.1	5.6	9.0	13.7	103.0	8.1
PLC (mm/cm^3)									
PLC $_{10\text{-}100}$	5025	454 (8.29)	283123.1±175247.6	19149.8	168233.5	243513.2	346557.4	1710893.0	178323.9
PLC $_{10\text{-}30}$	5025	454 (8.29)	66055.2±40376.0	5122.0	40110.3	56962.3	81370.0	961207.8	41259.7
PLC $_{30\text{-}100}$	5025	454 (8.29)	217067.9±143871.5	13461.7	124547.4	184315.4	266416.4	1528987.0	141869.0
PLC $_{100\text{-}500}$	5016	463 (8.45)	258871.0±175416.6	0.0	146015.9	222491.3	321293.0	1990223.0	175277.1
PLC $_{10\text{-}500}$	5016	463 (8.45)	542288.9±328150.2	46278.4	331981.8	472471.3	656972.5	3389249.0	324990.7
PSC (μm^2/cm^3)									
PSC $_{10\text{-}100}$	5025	454 (8.29)	46.0±29.8	3.3	26.6	39.2	56.7	311.9	30.1
PSC $_{10\text{-}30}$	5025	454 (8.29)	4.3±2.7	0.3	2.6	3.7	5.3	71.1	2.7
PSC $_{30\text{-}100}$	5025	454 (8.29)	41.7±27.8	2.7	23.7	35.4	51.4	299.1	27.7
PSC $_{100\text{-}500}$	5016	463 (8.45)	165.9±118.7	0.0	90.1	140.8	207.0	1430.6	116.9
PSC $_{10\text{-}500}$	5016	463 (8.45)	212.0±141.8	7.5	121.1	181.9	260.8	1685.5	139.7

Note: All air pollutants and meteorology were consecutively measured between 2006 and 2020 (5479 days). The values were calculated based on the original UFP data, excluding missing values (missing rate=8.29%-8.45%).

Abbreviations

N, number days with non-missing values; SD, standard deviation; IQR, interquartile range; PNC, particle number concentration; PMC, particle mass concentration; PLC, particle length concentration; PSC, particle surface concentration; 10–100, from 10 to 100 nm mobility diameter; 10–30, from 10 to 30 nm mobility diameter; 30–100, from 30 to 100 nm mobility diameter; 100–500, from 100 to 500 nm mobility diameter; 10–500, from 10 to 500 nm mobility diameter.

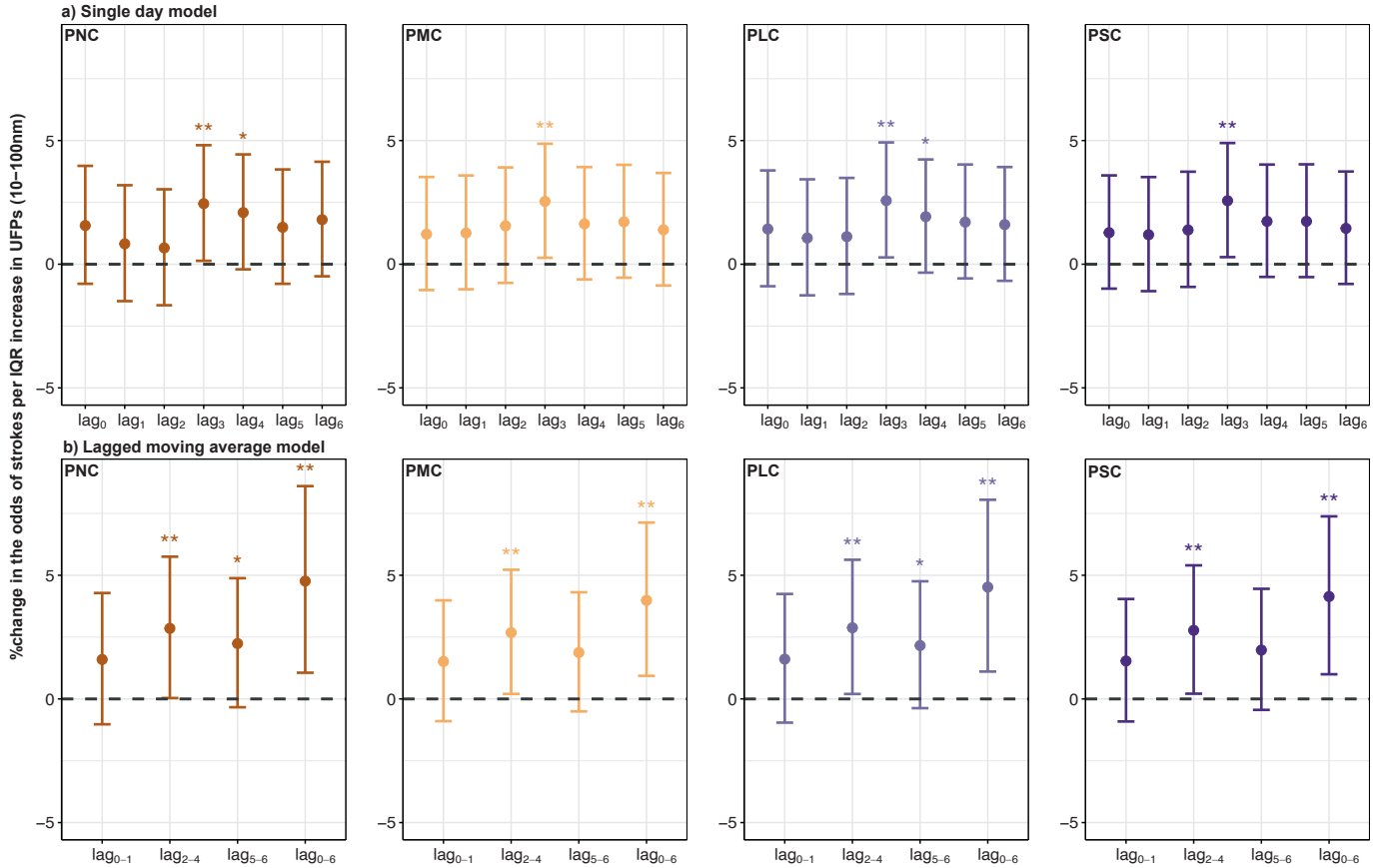

Fig. 1. Percent change (95 %CI) in the odds of overall stroke events per interquartile range (IQR) increase in the a) single-day and b) lagged moving average UFP metrics (10–100 nm). Note: * $P < 0.10$; ** $P < 0.05$.

the range of 10–100 nm on stroke events. Across four UFP metrics, we found for lag 0–6 the strongest impact of $PNC_{10\text{-}100}$ on strokes (PC = 4.76 % [1.06; 8.60]), followed by $PLC_{10\text{-}100}$ (PC = 4.52 % [1.11; 8.05]), and $PSC_{10\text{-}100}$ (PC = 4.14 % [1.00; 7.38]), with the weakest impact being found for $PMC_{10\text{-}100}$ (PC = 3.99 % [0.93; 7.13]) (see sTable 7).

As most of the effects across the four metrics were consistently observed at the lag of 3 and 0–6 days, these exposure windows were consequently used as the main lag periods for secondary analyses. When comparing the four size-fractioned UFPs in association with strokes, we noticed that the patterns of associations were similar and comparable across the four metrics (Fig. 2). Within the ultrafine range (10–100 nm), it is noteworthy that the effects of particles from the Aitken mode (30–100 nm) were more robust than the smaller particles from the nucleation mode (10–30 nm) between the two exposure windows. The effects of large particles in the accumulation mode (100–500 nm) were less stable than particles in other size ranges (data are available in sTables 6&7).

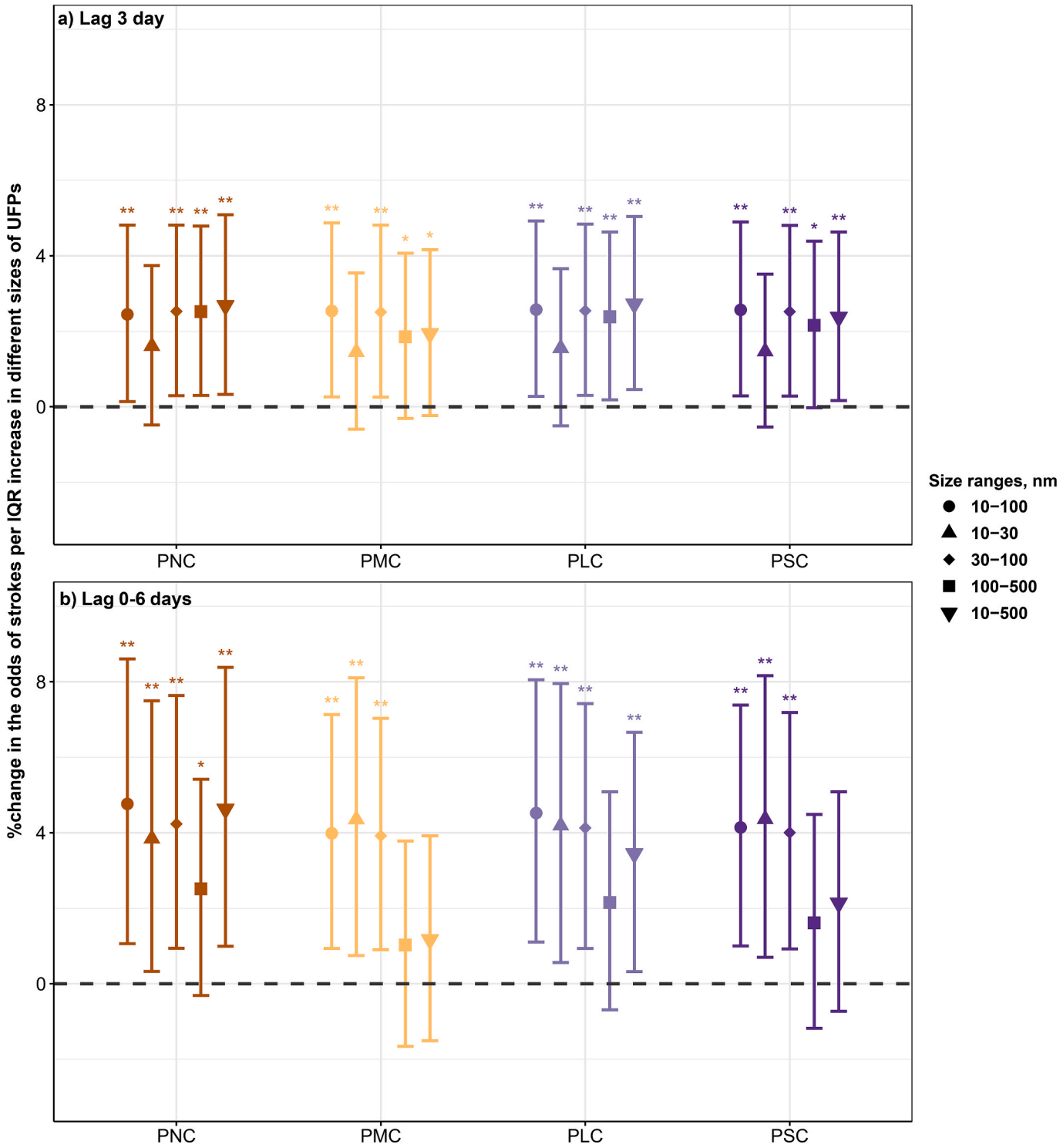

Fig. 2. Percent change (95 %CI) in the odds of overall stroke events per interquartile range (IQR) increase in five sizes of a) lag 3 and b) 0–6 days of UFP metrics. Note: * $P < 0.10$; ** $P < 0.05$.

3.3. Stratified analyses

When dividing stroke patients by their sub-types, the adverse health effects of UFPs on strokes were mostly found for patients with ischemic strokes, which were significantly associated with the cumulative 0–6 days of $PMC_{10\text{-}100}$ (3.83 % [0.15; 7.64]), $PLC_{10\text{-}100}$ (PC = 4.16 % [0.08; 8.42]), and $PSC_{10\text{-}100}$ (PC = 3.91 % [0.13; 7.83]) (Fig. 3). Aside from the UFPs (10–100 nm), ischemic stroke patients were more vulnerable to PMC, PLC, and PSC from the Aitken mode (30–100 nm) than UFPs in other sizes in the exposure window of lag 0–6 days (sFigs. 5–8). Numeric data are available in sTable 8.

The stratification by stroke-induced disability revealed that the effect

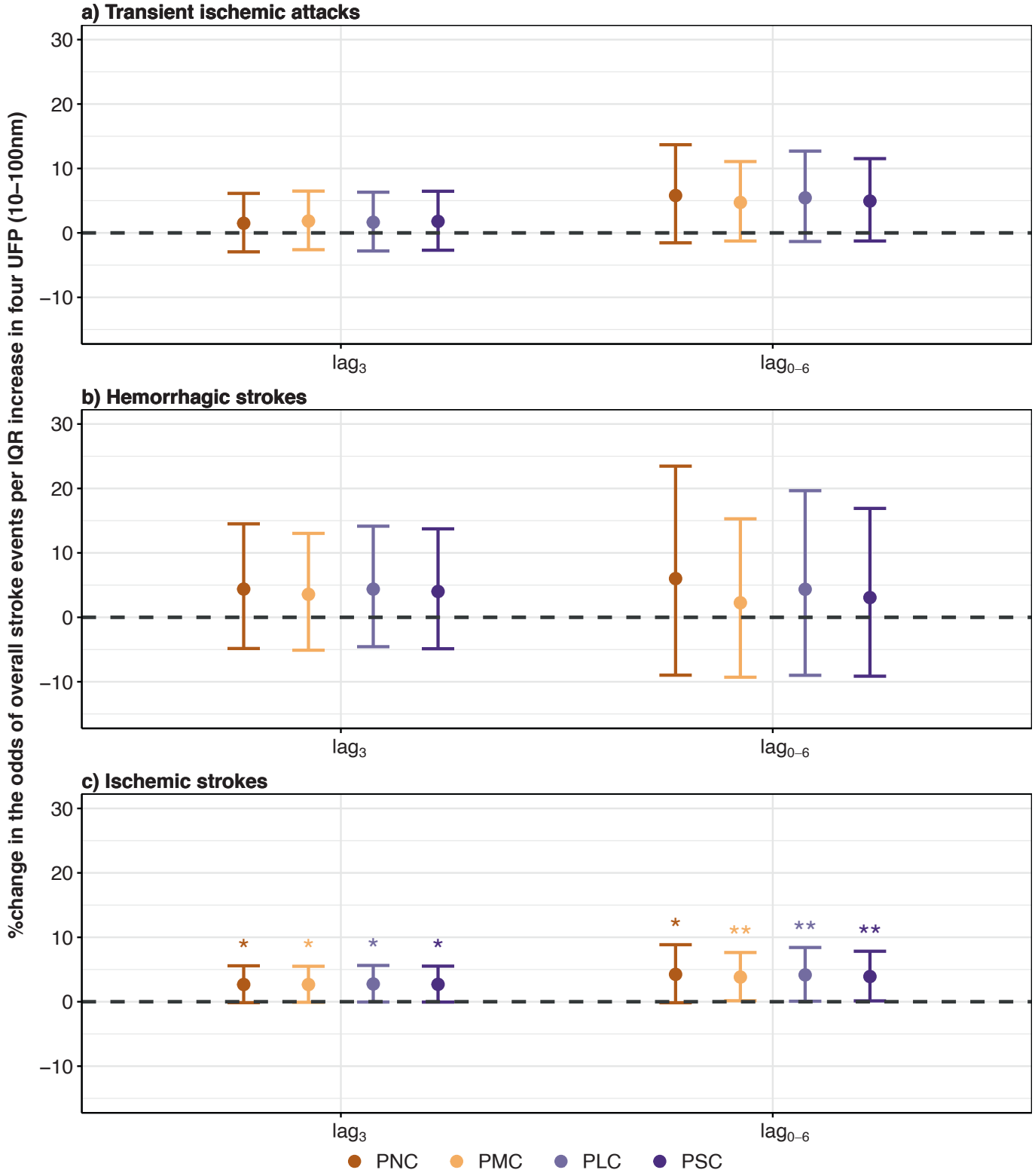

Fig. 3. Percent change (95 %CI) in the odds of three stroke subtypes per interquartile range (IQR) increase in lag 3 and 0–6 days of UFP metrics (10–100 nm). Note: * $P < 0.10$; ** $P < 0.05$.

of lagged moving average 0–6 days of $PNC_{10\text{-}100}$ was more pronounced among patients with slight disability levels (No symptoms to slight disability) (see sFig. 9 & sTable 9). Comparable patterns were identified for the stratification by stroke severity, with the effect estimates for lag 0–6 days of $PNC_{10\text{-}100}$ and $PLC_{10\text{-}100}$ being stronger among patients with milder stroke severity (No symptoms to minor stroke) (see sFig. 10 & sTable 10). In particular, we noticed that the effects of all UFP metrics from the nucleation mode (10–30 nm) were larger among patients with a milder disability or severity than their more severe counterparts.

3.4. Effect modification

Generally, as presented in sTables 11–13, the association between four UFP metrics (10–100 nm) in two exposure windows did not vary significantly across sex, age, seasons, and five-year periods, but the cold spells of ETEs seem to modify the effect of UFPs on strokes. Although no significant effect modification was noticed for seasons or ETEs, the adverse effects of UFPs (10–100 nm) in triggering stroke events were stronger during cold spells within the cold seasons (sTable 12). Under

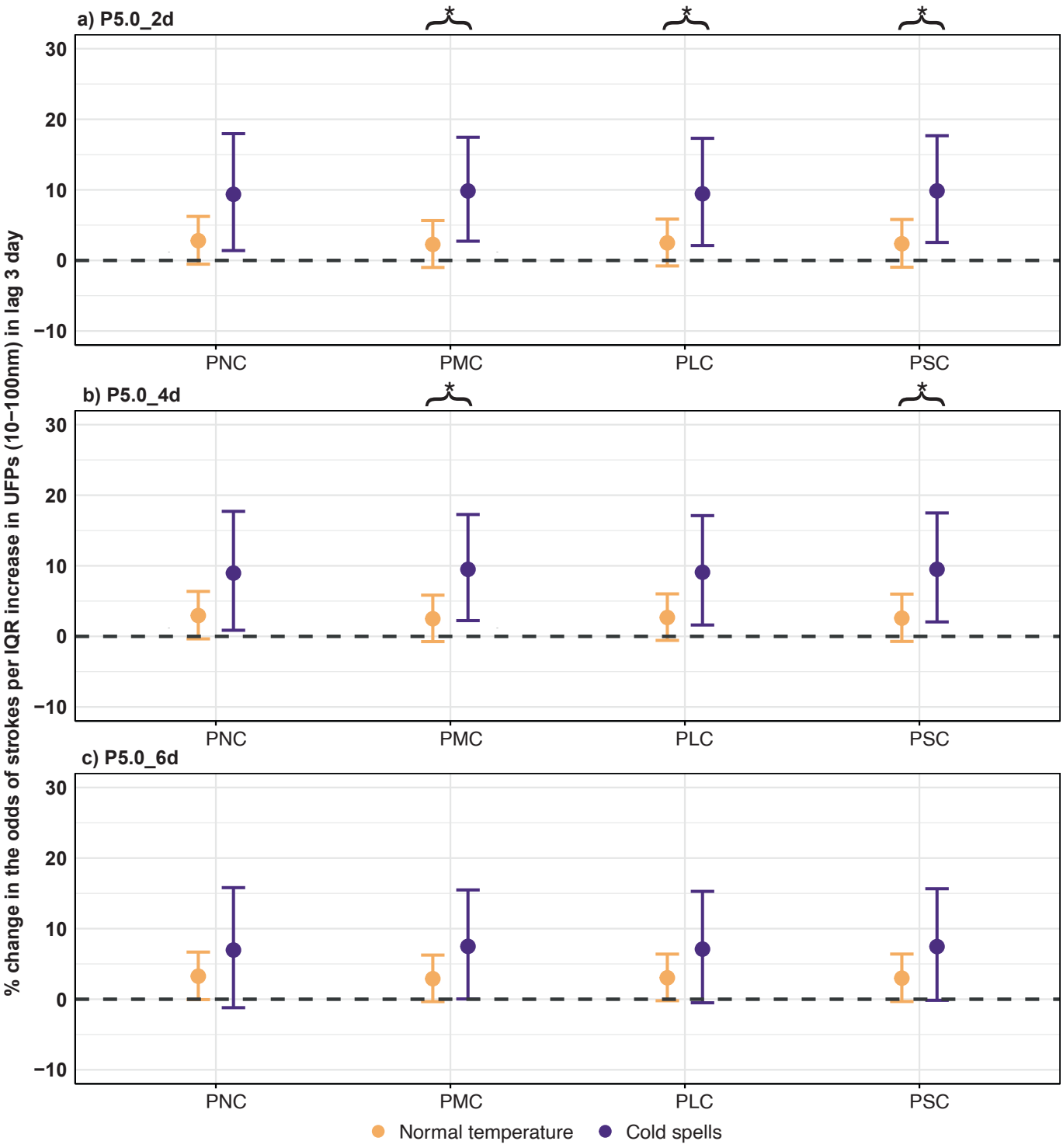

Fig. 4. Effect modification by the consecutive a) 2 days, b) 4 days, and c) 6 days of P5.0 thresholds of cold spells on the association between lag 3 days of UFP metrics (10–100 nm) and the percent changes in the odds of overall stroke events. Note: * *P*-interaction < 0.10.

the definitions of P5.0_2d or P5.0_4d of the cold spells, the lag 3-day exposures to PMC_{10-100}, PLC_{10-100}, and PSC_{10-100} displayed stronger effects on stroke events compared to the days with normal air temperature (*P*-interaction < 0.10) (Fig. 4), with the modification effect of the P5.0 threshold of cold spells being attenuated with longer durations. In contrast, we did not observe any modification effect of cold spells on the effects of four metrics for lag 0–6 days (sFig. 11), and no modification effect was observed for exposure to heat waves under different definitions during warm seasons, regardless of exposure windows (sFigs. 12–13, sTable 13).

3.5. Sensitivity analyses

In the two-pollutant models, the results of lag 0–6 days UFPs (10–100 nm) remained stable after additional adjustment for selected co-pollutants. By contrast, the effects of UFP exposures at a lag of 3 days were slightly attenuated after the adjustments for NO_2, which shares similar sources with UFPs (Ohlwein et al., 2019) (see sFigs. 14–15 & sTable 14). In addition, the significant associations between overall stroke events and UFPs (10–100 nm) at the lag 3 day and lag 0–6 days persisted in the models that used the imputed data, excluded patients diagnosed with strokes after the beginning of COVID-19 pandemic, as well as adjusted for high and low temperatures (sFigs. 16–17 & sTable 15).

The exposure–response functions between the four metrics (10–100 nm) and overall stroke events during the lag 3 day and 0–6 days are illustrated in sFigs. 18 & 19. Based on the likelihood ratio test, no deviation from linearity was observed for all four metrics in the two exposure windows, with the likelihood ratio test consistently indicating no differences between linear and non-linear models (all *P*-values for the likelihood ratio test >0.05).

4. Discussion

In this 15-year population-based study, we found the delayed and cumulative adverse effects of UFP metrics (10–100 nm) on strokes, with the effect estimates for IQR increases in four metrics being comparable. Particles in the Aitken mode (30–100 nm) showed more consistent and positive associations with strokes than in the nucleation mode (10–30 nm). Furthermore, UFPs were more likely to adversely affect patients with ischemic and minor strokes. The UFP effects might be amplified during days with extremely low temperatures.

These results were consistent with supporting evidence of the detrimental health effects of UFPs, such as increased hospital admissions for diseases in the respiratory, cardiovascular, and neurological systems (Ohlwein et al., 2019; Schraufnagel, 2020; Abdul-Rahman et al., 2024). There is crosstalk between the heart and brain, facilitated by their physiological and neurohumoral complex networks (Fan et al., 2024). However, in comparison to the literature linking short-term exposure to ambient UFP with heart diseases (Chen et al., 2020; Jiang et al., 2023; Wolf et al., 2015; Hu et al., 2020), the evidence regarding strokes is sparse. So far, an early study in Helsinki, Finland (1998–2004) underscored a positive but insignificant association between the previous-day level of UFP and stroke mortality (8.5 % [-1.2; 19.1]) (Kettunen et al., 2007). Subsequently, another study in Copenhagen, Denmark (2003–2006) found that IQR increases in UFP at lag 4 days increased the risk of mild stroke by 14.0 % (4.0; 25.0) and the risk of ischemic strokes without atrial fibrillation by 9.0 % (1.0; 17.0) (Andersen et al., 2010). There is even less evidence focusing on different UFP metrics. The increased MI risks in response to hourly exposures to PLC and PSC were larger than for PNC, within the ultrafine range of 10–100 nm (Chen et al., 2020). Another study found that PSC might be a more sensitive indicator than PNC regarding the association with hospital admissions for cardiovascular diseases in New York State, U.S. (2013–2018) (Lin et al., 2022). Contrarily, we saw comparable effects across four UFP metrics across particle size distribution. This means that, aside from commonly used metrics (PNC and PMC), the physical characteristics of UFPs (PLC and PSC) might be additional indicators measuring the health impairment of UFPs. We hypothesize that particle toxicity and the biological pathways linking UFPs to strokes might be driven more by intrinsic properties (e.g., chemical composition) rather than size-specific characteristics (sizes or metrics), but we were unable to clarify this due to the unavailability of particulate chemical composition data. Notably, the strong correlations between the UFP metrics prevented us from separating their individual effects or assessing whether the high PNC in the 10–30 nm range compensated for lower PMC, PLC, and PSC, leading to similar overall results. Of note, the health effects of PMC warrant further investigation, as only a limited fraction of PMC can be measured within the conventional size threshold of 100 nm (Kwon et al., 2020). This measurement constraint hampers a comprehensive assessment of their potential impact on stroke risk. More studies are needed to further distinguish their effects and assess whether PMC, PSC, and PLC can fully capture the health-relevant aspects of UFPs.

Some studies have detected the variations in health effects of UFP metrics due to size fractions, but their findings have remained inconclusive. For instance, a time-series study in the Ruhr Area, Germany, showed that size-specific PNC (100–750 nm) and lung-deposited PSC had similar immediate and delayed associations with increased natural and cardiovascular mortalities, with PNC (100–500 nm) having the strongest effect on natural mortality (Hennig et al., 2018). Larger PNC, especially particles in the ranges of 30–100 nm and 100–800 nm, had stronger effects on hospital admissions for heart diseases, cardiovascular and respiratory diseases, compared to smaller size fractions (10–30 nm) (Schwarz et al., 2023). The effects of larger PNC on cardiovascular or respiratory hospital admissions were consistently reported by the observations in Prague, Czech Republic (≥346 nm *vs.* < 346 nm) (Braniš et al., 2010) and in Beijing, China (100–300 nm *vs.* < 100 nm) (Leitte et al., 2011). However, a study in Augsburg, Germany, reported a more precise positive association with MI for UFPs (30–100 nm), compared to the particles in the smaller or larger size range (Chen et al., 2020). Our size-fractioned analyses showed that particles in the ranges of 10–100 nm and 30–100 nm were more consistently associated with increased stroke risk than other modes across all four UFP metrics. The heterogeneity in findings across studies may be attributed to variations in the methodological issues and emission sources across study areas (Gu et al., 2012; HEI Review Panel on Ultrafine Particles, 2013). The diffusion coefficients and measurement uncertainty of particle size distribution measurement below 30 nm are high (Gu et al., 2012). This means that the bulk of the daily average UFP was detected in the size range above 30 nm, which yielded higher exposure levels and more precise effect estimates in the Aitken mode than those in the nucleation mode. Local variation of particles of this size cannot be ruled out because they are significantly affected by their proximity to major roads and peak traffic times (Gu et al., 2012; Gu et al., 2011). Despite this, particles within the range of 10–100 nm mainly reflect emissions from the diesel-driven motor vehicles in Augsburg (Gu et al., 2012), but massive amounts of airborne particles in the range of 100–500 nm are associated with stationary combustion, which is influenced by the use of residential heating facilities (Gu et al., 2011). These may partly explain the inconsistent results from this size range. In addition to metrics, we found stable and consistent associations of particles in the Aitken mode (30–100 nm) with strokes in both delayed mode (lag 3) and cumulative mode (lag 0–6), but the association of the smallest particles (nucleation mode, 10–30 nm) was only found at lag 0–6 days. This suggests that larger particles in the Aitken mode may exert effects after shorter exposure lags than their smaller counterpart in the nucleation mode. This finding needs to be interpreted with caution due to the methodological difficulties in measuring particles in this size fraction of UFPs.

There are direct and indirect pathways of UFPs being thought to trigger acute cerebrovascular stroke. Direct pollutant effects are hypothesized because inhaled UFPs are unique in their small size and high concentration, which enables them to deposit and retain in the distal

airways and alveoli, and enter the brain through the olfactory nerve, or enable them to penetrate the alveolar-capillary barrier, cross the blood–brain barrier, and subsequently gain access to the central nervous system, thus causing platelet aggregation and neuroinflammation (Abdul-Rahman et al., 2024; Chen et al., 2024; Underwood, 2017; Daiber et al., 2020; Kulick et al., 2023). After being exposed to UFPs for a longer period, the cumulative toxic effect may be evoked as UFPs can cross the alveolar membranes and release toxins into the bloodstream upon depositing on the vascular endothelium, then modify the integrity of vascular tissue by eliciting a surge in local oxidative stress and inflammation, and facilitating plaque instability and thrombosis (Abdul-Rahman et al., 2024; Daiber et al., 2020). Convincing evidence has been presented that UFP exposure could access blood cells, elicit elevated blood levels of pro-inflammatory cytokines, and initiate the hepatic synthesis of acute-phase proteins (Aryal et al., 2021). The UFP-triggered oxidative stress would further promote vascular dysfunction and increase mitochondrial reactive oxygen species (ROS) formation and lipid oxidation (Abdul-Rahman et al., 2024). Excess ROS formation can influence blood pressure, accelerate atherosclerosis, and contribute to strokes (Abdul-Rahman et al., 2024; Daiber et al., 2020). By indirect pathways, the toxic effects of UFPs may be strengthened as their chemical constituent can cause not only vascular activation via producing circulating stress hormones and vasoconstrictors but also neuronal activation through autonomic lung arc reflexes or by a spillover of local inflammation into systemic inflammation (Daiber et al., 2020).

The risk of strokes associated with UFPs may vary depending on their subtypes and severity levels, with adverse effects predominantly found for ischemic strokes and minor strokes with a lower severity. There is supportive evidence of the positive association between short-term exposure to particulate air pollutants and ischemic stroke risk (Toubasi and Al-Sayegh, 2023), which are typically caused by the narrowing of vessels due to atherosclerosis or systemic embolism (Kuriakose and Xiao, 2020). Furthermore, our findings are in line with another study stating that strokes associated with UFP exposures were at the mild end of the stroke spectrum and probably resulted from blockages of small vessels (Andersen et al., 2010). Additionally, this may also relate to the "ceiling effect", in which additional UFP exposure may influence pathology already established over time but may fail to produce a detectable incremental effect when those with advanced disease have reached a plateau (Hennig et al., 2020). Given that the existing evidence on the biological mechanisms of particles in TIAs and hemorrhagic strokes remains insufficient, more investigations should attempt to elucidate their associations with UFPs.

The interaction model showed that the cold spells might modify the association, with the detrimental effects of UFPs on strokes being stronger in days with extreme cold air temperature, especially on the coldest 5.0 % of days lasting two or four days. As highlighted in previous research, the cold air temperature may amplify the adverse health effects of UFPs on the cardiovascular system, such as PSC-related hospitalizations (Lin et al., 2022) and PNC-related mortality (Chen et al., 2018). In particular, we noticed that the daily averages of four UFP metrics tended to increase during cold spells, as the levels increased when the cold spell cutoffs became more rigorous. We hypothesize that the excess risk of strokes in response to UFPs during cold spells may be attributed to elevated emissions of UFP from vehicles (Jeong et al., 2022), enhanced particle formation, and slower atmospheric dispersion under low air temperatures (HEI Review Panel on Ultrafine Particles, 2013; Sioutas et al., 2005). Likewise, as temperatures drop near ground level at night, stable atmospheric layers of air form, thus trapping primary pollutants near their emission sources (HEI Review Panel on Ultrafine Particles, 2013; Herner et al., 2006), thus amplifying their adverse health effects. No modification effect was observed for heat waves, so future studies are still needed to elucidate the effect of two sides of ETEs on strokes, especially under a changing climate.

This is the first study comparing the effects of four UFP metrics in different size fractions on stroke events. Besides, the validated and complete registration for strokes over 15 years enables us to systematically investigate the association of UFP exposure with strokes and their subtypes with sufficient statistical power. Moreover, the application of the case-crossover study design provides us with opportunities to control time-invariant factors. However, our study suffers from several limitations. First, the measurement of UFPs in our study relied on one fixed measuring site, which does not reflect the absolute concentrations, especially in near-source neighborhoods, such as next to busy roads and highways. However, short-term health effect studies are usually not biased by potential spatial variation, and a carefully selected monitoring site could be considered adequate for UFP because of the high temporal correlations of PNC across the city area of Augsburg (Cyrys et al., 2008). Clinically, conducting local analyses can identify warning signs of local environmental exposure, allowing healthcare professionals to better prepare for environmental pollution levels and stroke influxes. Second, it is challenging for us to differentiate the health effects of the four UFP metrics because they are highly correlated with each other. In general, the four UFP metrics exhibit largely consistent associations with strokes, indicating a certain level of comparability among these metrics. Third, there may be potential misclassification of reported TIAs, as their diagnosis is often challenging; transient symptoms may resolve quickly and are not always confirmed by imaging, meaning they might not result from a cerebral ischemic event. However, this would only cause reduced precision of associations in response to UFPs rather than blurring the real adverse effects. Finally, the generalizability of our findings to other populations is limited due to the potentially different demographic and socioeconomic characteristics and emission sources across study areas.

5. Conclusions

Short-term exposure to UFP may be associated with the occurrence of strokes, with similar effects observed across four UFP metrics, suggesting that PNC, PLC, and PSC may serve as promising indicators capturing the properties of UFPs. The detrimental impacts of UFPs were more pronounced for ischemic strokes and minor strokes with a lower severity. Particular attention should be directed toward particles within the range of 10–100 nm and those classified under the Aitken mode (30–100 nm). Notably, cold spells may amplify the damage of UFPs. More efforts are needed to monitor UFPs and to set up control levels, especially during days with extremely low air temperatures, thus alleviating the stroke burden.

CRediT authorship contribution statement

Minqi Liao: Writing – original draft, Visualization, Validation, Formal analysis. **Siqi Zhang:** Validation, Software, Formal analysis. **Maximilian Schwarz:** Visualization, Formal analysis. **Cheng He:** Visualization, Formal analysis. **Susanne Breitner-Busch:** Writing – review & editing. **Josef Cyrys:** Writing – review & editing. **Markus Naumann:** Writing – review & editing. **Lino Braadt:** Writing – review & editing. **Claudia Traidl-Hoffmann:** Writing – review & editing. **Gertrud Hammel:** Writing – review & editing. **Annette Peters:** Writing – review & editing, Supervision. **Michael Ertl:** Writing – review & editing, Methodology, Conceptualization. **Alexandra Schneider:** Writing – review & editing, Supervision, Methodology, Conceptualization.

Declaration of competing interest

The authors declare that they have no known competing financial interests or personal relationships that could have appeared to influence the work reported in this paper.

Acknowledgments

This work was supported by the scholarship under the Scholarship

Fund by the China Scholarship Council (File No. 202106780004). We are thankful to the staff and the patients at the University Hospital Augsburg.

Appendix A. Supplementary material

Supplementary data to this article can be found online at https://doi.org/10.1016/j.envint.2025.109823.

Data availability

Data will be made available on request.

References

Abdul-Rahman, T., Roy, P., Bliss, Z.S.B., et al., 2024. The impact of air quality on cardiovascular health: a state of the art review. Curr. Probl. Cardiol. 49 (2), 102174. https://doi.org/10.1016/j.cpcardiol.2023.102174.

Andersen, Z.J., Olsen, T.S., Andersen, K.K., Loft, S., Ketzel, M., Raaschou-Nielsen, O., 2010. Association between short-term exposure to ultrafine particles and hospital admissions for stroke in Copenhagen, Denmark. Eur. Heart J. 31 (16), 2034–2040. https://doi.org/10.1093/eurheartj/ehq188.

Aryal, A., Harmon, A.C., Dugas, T.R., 2021. Particulate matter air pollutants and cardiovascular disease: strategies for intervention. Pharmacol. Ther. 223, 107890. https://doi.org/10.1016/j.pharmthera.2021.107890.

Ban, J., Cheng, J., Zhang, C., et al., 2024. China's carbon-neutral policies will reduce short-term PM(2.5)-associated excess incidence of cardiovascular diseases. One Earth 7 (3), 497–505. https://doi.org/10.1016/j.oneear.2024.01.006.

Bergmann, M.L., Andersen, Z.J., Massling, A., et al., 2023. Short-term exposure to ultrafine particles and mortality and hospital admissions due to respiratory and cardiovascular diseases in Copenhagen, Denmark. Environ. Pollut. 336, 122396. https://doi.org/10.1016/j.envpol.2023.122396.

Braniš, M., Vyškovská, J., Malý, M., Hovorka, J., 2010. Association of size-resolved number concentrations of particulate matter with cardiovascular and respiratory hospital admissions and mortality in Prague, Czech Republic. Inhal. Toxicol. 22 (Suppl 2), 21–28. https://doi.org/10.3109/08958378.2010.504758.

Chen, J., Lai, X., Song, Y., Su, X., 2024. Neuroimmune recognition and regulation in the respiratory system. Eur. Respir. Rev. 33 (172).

Chen, R., Lu, J., Yu, Q., et al., 2015. The acute effects of outdoor temperature on blood pressure in a panel of elderly hypertensive patients. Int. J. Biometeorol. 59 (12), 1791–1797.

Chen, K., Wolf, K., Breitner, S., et al., 2018. Two-way effect modifications of air pollution and air temperature on total natural and cardiovascular mortality in eight European urban areas. Environ. Int. 116, 186–196. https://doi.org/10.1016/j.envint.2018.04.021.

Chen, K., Schneider, A., Cyrys, J., et al., 2020. Hourly exposure to ultrafine particle metrics and the onset of myocardial infarction in Augsburg, Germany. Environ. Health Perspect. 128 (1), 17003. https://doi.org/10.1289/ehp5478.

Cyrys, J., Pitz, M., Heinrich, J., Wichmann, H.E., Peters, A., 2008. Spatial and temporal variation of particle number concentration in Augsburg, Germany. Sci. Total. Environ. 401 (1–3), 168–175. https://doi.org/10.1016/j.scitotenv.2008.03.043.

Daiber, A., Kuntic, M., Hahad, O., et al., 2020. Effects of air pollution particles (ultrafine and fine particulate matter) on mitochondrial function and oxidative stress - implications for cardiovascular and neurodegenerative diseases. Arch. Biochem. Biophys. 696, 108662. https://doi.org/10.1016/j.abb.2020.108662.

Deng, B., Zhu, L., Zhang, Y., et al., 2024. Short-term exposure to PM(2.5) constituents, extreme temperature events and stroke mortality. Sci. Total Environ. 954, 176506. https://doi.org/10.1016/j.scitotenv.2024.176506.

Fan, X., Cao, J., Li, M., et al., 2024. Stroke related brain-heart crosstalk: pathophysiology, clinical implications, and underlying mechanisms. Adv Sci (weinh) 11 (14), e2307698. https://doi.org/10.1002/advs.202307698.

Gouveia, N., Rodriguez-Hernandez, J.L., Kephart, J.L., et al., 2024. Short-term associations between fine particulate air pollution and cardiovascular and respiratory mortality in 337 cities in Latin America. Sci. Total Environ. 920, 171073. https://doi.org/10.1016/j.scitotenv.2024.171073.

Gu, J., Pitz, M., Schnelle-Kreis, J., et al., 2011. Source apportionment of ambient particles: comparison of positive matrix factorization analysis applied to particle size distribution and chemical composition data. Atmos. Environ. 45 (10), 1849–1857. https://doi.org/10.1016/j.atmosenv.2011.01.009.

Gu, J., Pitz, M., Breitner, S., et al., 2012. Selection of key ambient particulate variables for epidemiological studies - applying cluster and heatmap analyses as tools for data reduction. Sci. Total Environ. 435–436, 541–550. https://doi.org/10.1016/j.scitotenv.2012.07.040.

He, C., Breitner, S., Zhang, S., et al., 2024. Nocturnal heat exposure and stroke risk. Eur. Heart J. 45 (24), 2158–2166. https://doi.org/10.1093/eurheartj/ehae277.

Health Effects Institute. State of Global Air 2024. Boston, MA: Health Effects Institute; 2024.

Hennig, F., Quass, U., Hellack, B., et al., 2018. Ultrafine and fine particle number and surface area concentrations and daily cause-specific mortality in the Ruhr Area, Germany, 2009-2014. Environ. Health Perspect. 126 (2), 027008. https://doi.org/10.1289/ehp2054.

HEI Review Panel on Ultrafine Particles, 2013. Ultrafine Particles. Understanding the Health Effects of Ambient Ultrafine Particles. In: HEI Perspectives, ed. 3. Health Effects Institute, Boston, Massachusetts.

Hennig, F., Geisel, M.H., Kälsch, H., et al., 2020. Air pollution and progression of atherosclerosis in different vessel beds-results from a prospective cohort study in the Ruhr Area, Germany. Environ. Health Perspect. 128 (10), 107003. https://doi.org/10.1289/ehp7077.

Herner, J.D., Ying, Q., Aw, J., Gao, O., Chang, D.P., Kleeman, M.J., 2006. Dominant mechanisms that shape the airborne particle size and composition distribution in central California. Aerosol Sci. Tech. 40 (10), 827–844.

Hinds, W.C., 1982. Aerosol technology: Properties, behavior, and measurement of airborne particles(Book). Wiley-Interscience, New York, 1982, 442 p 1982.

Hu, J., Tang, M., Zhang, X., et al., 2020. Size-fractionated particulate air pollution and myocardial infarction emergency hospitalization in Shanghai, China. Sci. Total Environ. 737, 140100. https://doi.org/10.1016/j.scitotenv.2020.140100.

Janes, H., Sheppard, L., Lumley, T., 2005. Case-crossover analyses of air pollution exposure data: referent selection strategies and their implications for bias. Epidemiology 16 (6), 717–726. https://doi.org/10.1097/01.ede.0000181315.18836.9d.

Jeong, C.H., Hilker, N., Wang, J.M., et al., 2022. Characterization of winter air pollutant gradients near a major highway. Sci. Total Environ. 849, 157818. https://doi.org/10.1016/j.scitotenv.2022.157818.

Jiang, Y., Chen, R., Peng, W., et al., 2023. Hourly ultrafine particle exposure and acute myocardial infarction onset: an individual-level case-crossover study in Shanghai, China, 2015-2020. Environ. Sci. Technol. 57 (4), 1701–1711. https://doi.org/10.1021/acs.est.2c06651.

Kasner, S.E., 2006. Clinical interpretation and use of stroke scales. Lancet Neurol. 5 (7), 603–612. https://doi.org/10.1016/s1474-4422(06)70495-1.

Kettunen, J., Lanki, T., Tiittanen, P., et al., 2007. Associations of fine and ultrafine particulate air pollution with stroke mortality in an area of low air pollution levels. Stroke 38 (3), 918–922. https://doi.org/10.1161/01.STR.0000257999.49706.3b.

Kim, J.H., 2019. Multicollinearity and misleading statistical results. Korean J. Anesthesiol. 72 (6), 558–569. https://doi.org/10.4097/kja.19087.

Kim, K.H., Kabir, E., Kabir, S., 2015. A review on the human health impact of airborne particulate matter. Environ. Int. 74, 136–143. https://doi.org/10.1016/j.envint.2014.10.005.

Kulick, E.R., Kaufman, J.D., Sack, C., 2023. Ambient air pollution and stroke: an updated review. Stroke 54 (3), 882–893. https://doi.org/10.1161/strokeaha.122.035498.

Kuriakose, D., Xiao, Z., 2020. Pathophysiology and treatment of stroke: present status and future perspectives. Int. J. Mol. Sci. 21 (20). https://doi.org/10.3390/ijms21207609.

Kwon, H.S., Ryu, M.H., Carlsten, C., 2020. Ultrafine particles: unique physicochemical properties relevant to health and disease. Exp. Mol. Med. 52 (3), 318–328. https://doi.org/10.1038/s12276-020-0405-1.

Lanzinger, S., Schneider, A., Breitner, S., et al., 2016. Ultrafine and fine particles and hospital admissions in central Europe. Results from the UFIREG Study. Am. J. Respir. Crit. Care Med. 194 (10), 1233–1241. https://doi.org/10.1164/rccm.201510-2042OC.

Leitte, A.M., Schlink, U., Herbarth, O., et al., 2011. Size-segregated particle number concentrations and respiratory emergency room visits in Beijing, China. Environ. Health Perspect. 119 (4), 508–513. https://doi.org/10.1289/ehp.1002203.

Lin, T.C., Chiueh, P.T., Hsiao, T.C., 2025. Challenges in observation of ultrafine particles: addressing estimation miscalculations and the necessity of temporal trends. Environ. Sci. Technol. 59 (1), 565–577. https://doi.org/10.1021/acs.est.4c07460.

Lin, S., Ryan, I., Paul, S., et al., 2022. Particle surface area, ultrafine particle number concentration, and cardiovascular hospitalizations. Environ. Pollut. 310, 119795. https://doi.org/10.1016/j.envpol.2022.119795.

Morawska, L., Ristovski, Z., Jayaratne, E., Keogh, D.U., Ling, X., 2008. Ambient nano and ultrafine particles from motor vehicle emissions: Characteristics, ambient processing and implications on human exposure. Atmos. Environ. 42 (35), 8113–8138. https://doi.org/10.1016/j.atmosenv.2008.07.050.

Ni, W., Stafoggia, M., Zhang, S., et al., 2024. Short-term effects of lower air temperature and cold spells on myocardial infarction hospitalizations in Sweden. J. Am. Coll. Cardiol. 84 (13), 1149–1159. https://doi.org/10.1016/j.jacc.2024.07.006.

Oberdörster, G., Oberdörster, E., Oberdörster, J., 2005. Nanotoxicology: an emerging discipline evolving from studies of ultrafine particles. Environ. Health Perspect. 113 (7), 823–839. https://doi.org/10.1289/ehp.7339.

Ohlwein, S., Kappeler, R., Kutlar Joss, M., Künzli, N., Hoffmann, B., 2019. Health effects of ultrafine particles: a systematic literature review update of epidemiological evidence. Int. J. Public Health 64 (4), 547–559. https://doi.org/10.1007/s00038-019-01202-7.

Peters, A., Rückerl, R., Cyrys, J., 2011. Lessons from air pollution epidemiology for studies of engineered nanomaterials. J. Occup. Environ. Med. 53 (6 Suppl), S8–s13. https://doi.org/10.1097/JOM.0b013e31821ad5c0.

Rankin, J., 1957. Cerebral vascular accidents in patients over the age of 60 II. Prognosis. Scott Med. J. 2 (5), 200–215. https://doi.org/10.1177/003693305700200504.

Rückerl, R., Schneider, A., Hampel, R., et al., 2016. Association of novel metrics of particulate matter with vascular markers of inflammation and coagulation in susceptible populations -results from a panel study. Environ. Res. 150, 337–347. https://doi.org/10.1016/j.envres.2016.05.037.

Sager, T.M., Castranova, V., 2009. Surface area of particle administered versus mass in determining the pulmonary toxicity of ultrafine and fine carbon black: comparison to ultrafine titanium dioxide. Part. Fibre Toxicol. 6, 15. https://doi.org/10.1186/1743-8977-6-15.

Schraufnagel, D.E., 2020. The health effects of ultrafine particles. Exp. Mol. Med. 52 (3), 311–317. https://doi.org/10.1038/s12276-020-0403-3.

Schwarz, M., Schneider, A., Cyrys, J., Bastian, S., Breitner, S., Peters, A., 2023. Impact of ultrafine particles and total particle number concentration on five cause-specific hospital admission endpoints in three German cities. Environ. Int. 178, 108032. https://doi.org/10.1016/j.envint.2023.108032.

Schwarz, M., Schneider, A., Cyrys, J., Bastian, S., Breitner, S., Peters, A., 2023. Impact of ambient ultrafine particles on cause-specific mortality in three German cities. Am. J. Respir. Crit. Care Med. 207 (10), 1334–1344. https://doi.org/10.1164/rccm.202209-1837OC.

Sioutas, C., Delfino, R.J., Singh, M., 2005. Exposure assessment for atmospheric ultrafine particles (UFPs) and implications in epidemiologic research. Environ. Health Perspect. 113 (8), 947–955. https://doi.org/10.1289/ehp.7939.

Stafoggia, M., Samoli, E., Alessandrini, E., et al., 2013. Short-term associations between fine and coarse particulate matter and hospitalizations in Southern Europe: results from the MED-PARTICLES project. Environ. Health Perspect. 121 (9), 1026–1033. https://doi.org/10.1289/ehp.1206151.

Sun, Y., Milando, C.W., Spangler, K.R., et al., 2024. Short term exposure to low level ambient fine particulate matter and natural cause, cardiovascular, and respiratory morbidity among US adults with health insurance: case time series study. BMJ 384, e076322. https://doi.org/10.1136/bmj-2023-076322.

Toubasi, A., Al-Sayegh, T.N., 2023. Short-term exposure to air pollution and ischemic stroke: a systematic review and meta-analysis. Neurology 101 (19), e1922–e1932. https://doi.org/10.1212/wnl.0000000000207856.

Underwood, E., 2017. The polluted brain. American Association for the Advancement of Science; 2017.

Wichmann, H.E., Spix, C., Tuch, T., et al., 2000. Daily mortality and fine and ultrafine particles in Erfurt, Germany part I: role of particle number and particle mass. Res. Rep. (Health Effects Institute) 2000;98:5–86; discussion 7.

Wichmann, H.E., Spix, C., Tuch, T., et al., 2000. Daily mortality and fine and ultrafine particles in Erfurt, Germany part I: role of particle number and particle mass. Res. Rep. Health Eff. Inst. 98.

Wolf, K., Schneider, A., Breitner, S., et al., 2015. Associations between short-term exposure to particulate matter and ultrafine particles and myocardial infarction in Augsburg, Germany. Int. J. Hyg. Environ. Health 218 (6), 535–542. https://doi.org/10.1016/j.ijheh.2015.05.002.

Xu, R., Huang, S., Shi, C., et al., 2023. Extreme temperature events, fine particulate matter, and myocardial infarction mortality. Circulation 148 (4), 312–323. https://doi.org/10.1161/circulationaha.122.063504.

Yao, Y., Schneider, A., Wolf, K., et al., 2023. Longitudinal associations between metabolites and immediate, short- and medium-term exposure to ambient air pollution: results from the KORA cohort study. Sci. Total Environ. 900, 165780. https://doi.org/10.1016/j.scitotenv.2023.165780.

Yu, W., Xu, R., Ye, T., et al., 2024. Estimates of global mortality burden associated with short-term exposure to fine particulate matter (PM(2·5)). Lancet Planet Health 8 (3), e146–e155. https://doi.org/10.1016/s2542-5196(24)00003-2.

Zhang, S.-H., Flagan, R.C., 1996. Resolution of the radial differential mobility analyzer for ultrafine particles. J. Aerosol Sci 27 (8), 1179–1200. https://doi.org/10.1016/0021-8502(96)00036-5.